Available online at www.sciencedirect.com
SCIENCE DIRECT®
ELSEVIER
Palaeogeography, Palaeoclimatology, Palaeoecology 209 (2004) 141–154
PALAEO
www.elsevier.com/locate/palaeo

Paleoenvironments in Russkaya Gavan' Fjord (NW Novaya Zemlya, Barents Sea) during the last millennium

Ivar Murdmaa[a], Leonid Polyak[b,*], Elena Ivanova[a], Natalia Khromova[a]

[a] *Shirshov Institute of Oceanology, Russian Academy of Sciences, Nakhimovskii Prosp. 36, 117997 Moscow, Russia*
[b] *Byrd Polar Research Center, Ohio State University, Columbus, OH 43210, USA*

Abstract

The 6-m long sediment core ASV-987 was collected from the deep part of the glaciated Russkaya Gavan' Fjord at the northwestern coast of Novaya Zemlya, Barents Sea, in 1997 (r/v Akademik Sergei Vavilov). The core was investigated for lithology, grain size, coarse debris, organic carbon, foraminifera, macrobenthic remains, and stable isotopes in foraminiferal tests. Age control was provided by seven AMS ^{14}C ages. The recovered sedimentary section spans approximately 800 years, from ca. 1170 AD. The proxy records reveal variations in sedimentation processes, bioproductivity, glacier front position, sea-ice conditions, and the hydrographic regime in the fjord. These characteristics are interpreted in terms of regional and global climatic changes during the last millennium. We distinguish four stages in the development of sedimentary environments in Russkaya Gavan', which generally correspond to major climatic events: the Medieval Warm Period (MWP), the early and late phases of the Little Ice Age (LIA), and recent warming. The most pronounced change in sedimentation regime occurred at the onset of the LIA ca. 1400, presumably due to the advance of a glacier into the fjord. Subsequent evolution of sedimentary environments included stabilization and retreat of the glacier front. The most recent facies are interpreted to indicate a change towards warmer conditions.
© 2004 Elsevier B.V. All rights reserved.

Keywords: High arctic; Barents Sea; Fjord; Glaciomarine environment; Sedimentary record; Medieval Warm Period; Little Ice Age

1. Introduction

The evolution of climate during the past millennium includes several large-scale paleoclimatic events indicated at many locations in the Northern Hemisphere by multidisciplinary data sets including mountain glacier advances, historical and archaeological evidence, dendrochronological, palynological, oxygen isotope studies, and other paleoclimate proxies (e.g., Bradley and Jones, 1993; Jones et al., 2001; Bradley et al., 2003 and references therein). Notably, the generally coldest period between ca. 1400 and 1900 AD, known as the Little Ice Age (LIA), was preceded by the Medieval Warm Period (MWP) and followed by recent warming. Although there is considerable debate on the extent and timing of these events (Ogilvie and Jónsson, 2001), the evidence is growing that they were especially pronounced in areas surrounding the North Atlantic and were possibly connected with changes in the North Atlantic atmospheric and oceanic circulations (e.g., Grove, 2001; Jones et al., 2001).

* Corresponding author. Tel.: +1-614-292-2602; fax: +1-614-292-4697.
E-mail address: polyak.1@osu.edu (L. Polyak).

0031-0182/$ - see front matter © 2004 Elsevier B.V. All rights reserved.
doi:10.1016/j.palaeo.2004.02.020

Marine evidence for the most recent climatic change is limited, because marine sedimentary records are rarely sufficiently highly resolved to distinguish century and decadal-scale events. Nevertheless, records with sub-millennial resolution consistently indicate the pervasive effects of the MWP, LIA, and 20th century warming on oceanographic conditions at various sites around the North Atlantic (Jennings and Weiner, 1996; Keigwin, 1996; Keigwin and Pickart, 1999; De Menocal et al., 2000). A recent quest for high-resolution paleoceanographic records, notably by the IMAGES program, resulted in several sediment cores with century to decadal scale resolution on both sides of the North Atlantic (Andersen et al., 2003; Cronin et al., 2003). These records indicate broad intervals of oceanographic regimes corresponding to the MWP, two-phase LIA, and subsequent warming as well as rapid, decadal temperature and salinity changes. These data shed light on the patterns and mechanisms of climate change in the North Atlantic, but its relationship to the Arctic remains to be understood.

Our multiproxy study of the 6-m-long gravity core ASV-987 from Russkaya Gavan' Fjord, northwestern coast of Novaya Zemlya, provides the first sub-millennial sedimentary record from the eastern Barents Sea, which is located downstream the North Atlantic drift (Fig. 1). Major results of the study, including the geochronological data, are presented in the initial report (Polyak et al., 2004). Here we present more detailed results focusing on the response of glaciomarine environments in Russkaya Gavan' to large-scale climatic events of the last millennium.

2. Physiographic and oceanographic settings

Russkaya Gavan' (Russian Harbour) is a glacier-influenced fjord at the northwestern coast of the Novaya Zemlya archipelago (Fig. 1). It opens northwards to the Barents Sea with an 8-km-wide mouth and extends SSW about 11 km inland. The central steep-sloped trough of the fjord, contoured by a 100-m isobath, is connected to the open sea by two branches separated by a shallower bank. Two small depressions reaching about 175 m deep are located along the fjord axis. Core ASV-987 was collected in the southern depression from a water depth of 170 m.

The Shokal'ski Glacier drains into the fjord from its south-eastern end. Meltwater discharge is the only substantial source of fine-grained sedimentary material today, whereas, small icebergs and coastal sea ice distribute minor amounts of IRD throughout the fjord.

For over 60 years, Russkaya Gavan' was the site of a weather station, which provided one of the few meteorological archives for the eastern Barents Sea, an area of intense Arctic-Atlantic oceanic and atmospheric interactions. The glacial regime of Shokal'ski

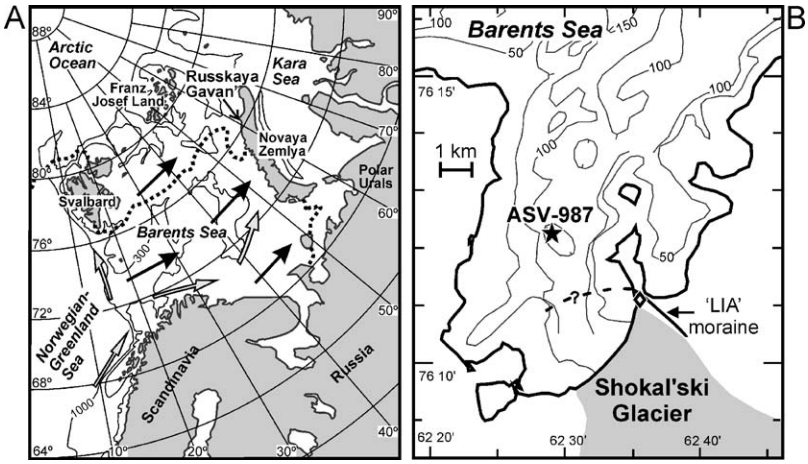

Fig. 1. (A) Map of the Barents Sea with 300- and 1000-m isobaths, minimal winter sea ice margin (dotted line), and direction of Atlantic water flows (grey arrows) and winter cyclones (black arrows). (B) Index map of Russkaya Gavan' with bathymetry in 50-m intervals. The diamond north of the glacier shows the location of a ^{14}C age constraint from the moraine (Zeeberg, 2001).

Glacier has been repeatedly studied since 1933 (Chizhov et al., 1968; Mikhaliov and Chizhov, 1970). These unique high-Arctic data sets, combined with high-resolution sedimentary archives associated with glaciomarine fjord environments, make Russkaya Gavan' a key site for studies of paleoclimatological and paleoceanographic changes in the Barents Sea.

The summer meltwater discharge strongly affects hydrographic conditions in the fjord by forming a stratified water column with low-salinity, suspension-rich surface water and saline, suspension-poor deep water that flows into the fjord from the open Barents Sea. The winter temperature regime is a likely control on ice and, thus, hydrographic conditions in Russkaya Gavan', as illustrated by the correlation between sea-ice melting time in spring and winter air temperatures (Mikhaliov and Chizhov, 1970). Winter temperatures reflect regional hydrographic and atmospheric patterns. This connection is demonstrated by a multi-decadal co-variation of winter air temperatures at the western side of Novaya Zemlya and water temperature and ice cover in the Barents Sea (Zeeberg and Forman, 2000).

As measured in September 1997, the concentration of suspended sediment in surface water varied from ~ 60 mg/l near the glacier front to 13.5 mg/l near ASV-987 and ~ 5 mg/l at the fjord mouth. By comparison, concentrations of up to 300 mg/l are measured in coastal meltwater flows (Aibulatov et al., 1999). Vertical distribution of suspended matter in the water column shows high concentrations above the strong pycnocline at about 25 m and within the near-bottom nepheloid layer separated by transparent intermediate water. This distribution pattern indicates lateral suspended sediment transport from the glacier discharge area by both surface currents and near-bottom flows.

Seismic reflection data show that stratified sediments overlying a hard reflector identified as a top of subglacial diamicton increase in thickness from several meters to much more than 30 m towards the glacier (Polyak et al., 2004). This ice-proximal sedimentary wedge consists of three units separated by strong reflectors, which possibly indicate the two most recent glacier advances. Near the ASV-987 site, stratified sediment comprises approximately 20 m. A 3.5 kHz 'Parasound' acoustic profile across the fjord trough demonstrates an acoustically laminated seismic unit that wedges out towards the steep slope of the trough (L. Merklin, personal communication).

The pattern of suspended-matter and bottom-sediment distribution along the fjord indicate that sedimentation in Russkaya Gavan' is largely controlled by the Shokalskii glacier meltwater, which constitutes the only significant sediment source in the fjord.

3. Materials and methods

The 6-m-long gravity core ASV-987 was raised by the r/v Akademik Sergei Vavilov in 1997 from the deepest central part of Russkaya Gavan' (76°12.25′ N, 62°29.19′ E, 170 m water depth) at a distance of ~ 5 km from the Shokalski Glacier front (Fig. 1). The core was described in detail visually and in smear slides immediately after raising. Then it was sampled in 5-cm intervals (samples 2 cm thick) for sand content, foraminiferal, and stable-isotope studies; a sparser sampling interval was used for other analyses including water content, bulk density, detailed grain size, total organic carbon (TOC) and carbonate contents, and clay minerals. Lithological and foraminiferal analyses were performed in the Shirshov Institute of Oceanology, Russian Academy of Sciences (SIO RAS). Age control was provided by seven AMS ^{14}C datings of mollusk shells performed at the Arizona AMS Facility (Polyak et al., 2004).

Detailed grain size distribution was analysed at intervals of 10–20 cm by applying a combined pipette and decantation method. Content of coarse fractions (>1, 1–0.1, and 0.1–0.05 mm) was determined at 5-cm intervals by washing and sieving. In order to adapt the decimal scale of size fractions traditionally used in Russia to western classifications based on logarithmical scale, we denote fractions less than 0.005 mm as clay, fractions 0.05–0.005 mm as silt, fractions 1–0.05 mm as sand, and those coarser than 1 mm as gravel (pebbles).

We examined the coarse sediment fraction >1 mm under a binocular microscope to evaluate semi-quantitatively a relative abundance of rock fragments, bivalve shells, and chitinous polychaeta tubes. Rock fragments >2 mm were counted per weight of dry sediment.

Foraminifers were counted and identified in the 0.1–1 mm fraction. When available, 200–400 tests of benthic foraminifera were counted in an appropriate

split aliquot of a sample. All planktonic foraminifera, typically occurring in minor amounts, were counted from the same aliquots. In samples containing only sparse foraminifers, all tests were counted.

Total organic carbon (TOC) and carbonate carbon were measured on a carbon analyzer AN-7529. Compositions of oxygen and carbon stable isotopes ($\delta^{18}O$ and $\delta^{13}C$) were simultaneously measured in tests of benthic foraminifer *Elphidium excavatum* forma *clavata* on a Finnigan MAT-252 mass-spectrometer at the Woods Hole Oceanographic Institution.

4. Results

4.1. Lithology and stratigraphy

Sediment in ASV-987 consists of olive gray and dark olive gray to black clay and silty clay with scattered gravel and pebbles unevenly distributed along the core. Sedimentary structures are represented by burrow mottling, indistinct (diffuse) layering, coarse or fine parallel lamination, and fine convolute lamination. Dark color shades result from the presence of iron monosulfides indicating reducing conditions during early diagenesis. Black iron-sulfide aggregates occur as burrow mottles, laminae, and interbeds. The sediment is very soft (soupy) in the upper 10 cm and becomes stiffer downward reaching very stiff in the core catcher. Water content decreases downcore and wet density increases correspondingly. However, the increase in density is not uniform throughout the core, but has several steps and some softer layers occur below the stiffer intervals.

We subdivided the core into four lithostratigraphic units, I–IV, based on changes in sedimentary structure, grain-size, coarse-fraction content and composition, and sedimentation rates estimated by interpolation between the ^{14}C ages (Fig. 2). The age constraint appears to be robust for units III–IV, below the 180-cm level dated to ca. 1600 AD (Polyak et al., 2004). Above this level, there are no ^{14}C ages except for the post-bomb dating at 45 cm. Therefore, the age model for units I–II is only tentative and may be subject to change if further age control is achieved.

Unit IV (4.45–5.96 m, ca. 1170–1400 AD) is composed of relatively stiff, dark olive-gray clay intercalated with diffuse darker interbeds (iron-sulfide enriched). The middle interval of this unit (4.84–5.25 m) is somewhat softer and distinctly laminated (black/gray interbeds). Throughout the unit, sediment contains angular rock fragments (mainly black shale), up to 15 mm in size. These are especially abundant below the level of 5.6 m. Linear sedimentation rates of around 0.6 cm/year are estimated for most of the unit length, though a region with double this rate (1.3 cm/year) extends into the upper part of this unit from above (Fig. 2).

Unit III (1.75–4.45 m, ca. 1400–1600 AD) is separated from the underlying unit IV by a distinct contact. Unit III comprises two laminated intervals with a diffusely layered bed in between (2.8–3.3 m, ca. 1470–1510 AD). Overall, unit III is characterized by the highest estimated sedimentation rates in the entire core (1.2–1.8 cm/year).

The 1.15-m-thick, coarsely laminated basal interval of unit III (3.3–4.45 m, ca. 1470–1400 AD) is composed of alternating black (0.5–5 cm thick) and gray (1–10 cm thick), silty clay laminae. In addition to this coarse lamination, a smear-slide observation from this interval indicates millimeter-scale, fine-sand laminae reflected in an overall elevated content (up to 4%) of fine sand (0.1–0.05 mm fraction). Gravel-size rock fragments are very unevenly distributed, fluctuating between zero and high concentrations. Estimated linear sedimentation rates in this interval are as high as 1.3–1.8 cm/year, but actual rates may have been even higher, because the datings used as tie points are located within adjacent, diffusely layered intervals, which are likely characterized by slower sedimentation (Fig. 2).

The upper meter of unit III (1.75–2.8 m, ca. 1510–1600 AD) has thin, millimeter-scale lamination, faint in the lower part of this interval (2.0–2.8 m) and distinct uppersection. Convolute lamination resembling that of bacterial mats occurs within the interval of 2.4–2.8 m. Above, unit III contains abundant subangular to subrounded rock fragments, up to 22 mm in diameter, represented by several varieties of sedimentary and, possibly, metamorphic rocks. The average linear sedimentation rate in the upper part of unit III is 1.2 cm/year (Fig. 2).

Unit II (0.96–1.75 m, ca. 1600–1800 or 1900 AD) is composed of olive-gray to dark olive-gray silty clay with diffuse, decimeter-scale lighter interbeds and

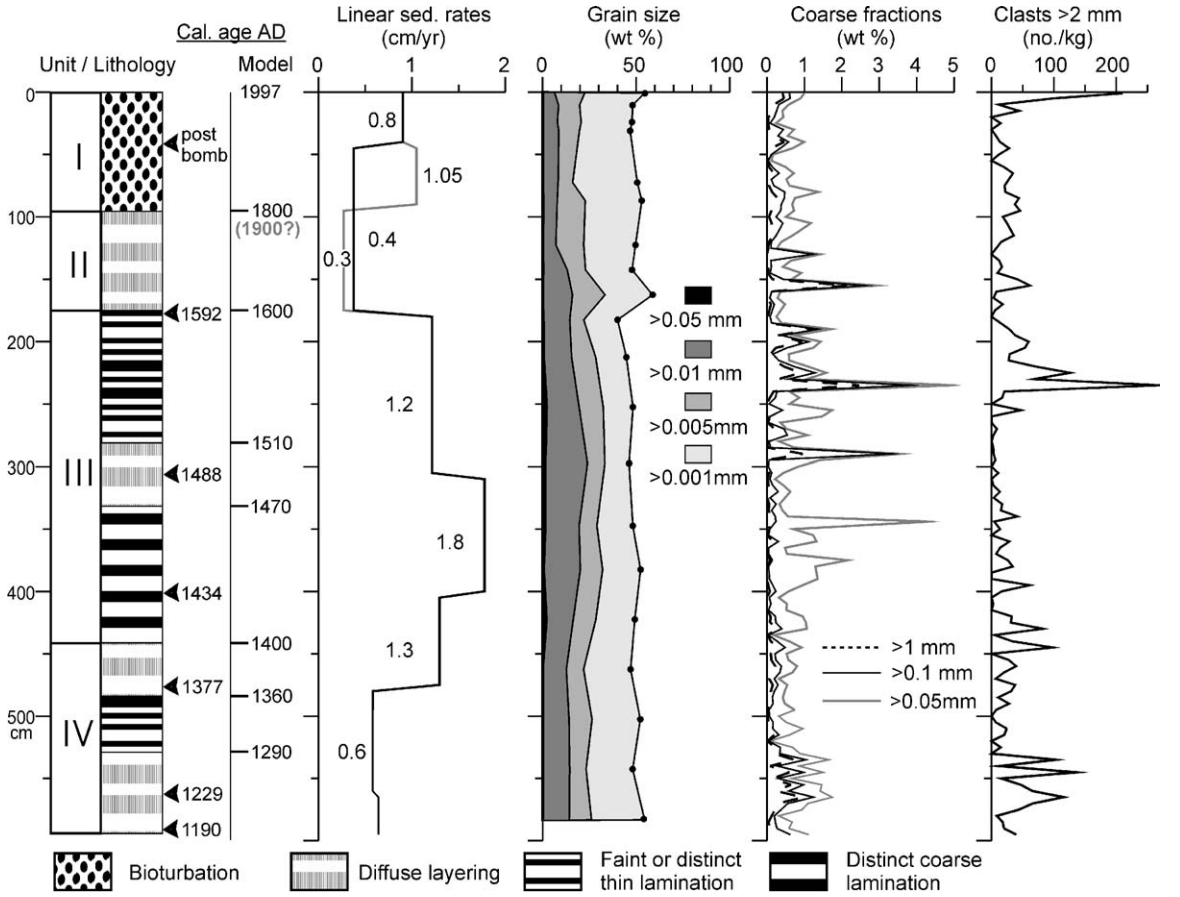

Fig. 2. Core ASV 987: stratigraphic subdivision, lithology, calibrated ^{14}C ages (determined and interpolated for unit boundaries), sedimentation rates estimated between the ^{14}C age determinations (two alternative models for units I and II), grain-size distribution, coarse fraction content (wt. %), and counted number of >2 mm rock clasts per 1 kg of dry sediment.

several centimeter-scale darker, iron-sulfide enriched layers. The sediment has mostly low coarse fraction contents, except for two levels that are relatively enriched in sand and gravel (Fig. 2). The transition from unit III to unit II is marked by the disappearance of distinct lamination and a dramatic, at least three-fold, decrease in sedimentation rate that occurred soon after ca. 1590 AD.

Unit I (0–0.96 m) is composed of intensely bioturbated (burrow mottled), very soft, olive-gray to dark olive-gray clay. The basal (0.8–0.96 m) and the top (0.1–0.45 m) intervals, except for the soupy surficial layer (0–0.1 m), are darker than the intervening sediment due to more abundant iron-sulfide stained burrows. For the most part, this sediment contains less than 1% coarse fractions. The content of rock fragments >2 mm is somewhat elevated in the lower part of the unit and rises noticeably in the surficial layer (Fig. 2).

The timing of the transition between units II and I is problematic because of a lack of ^{14}C determinations within these units other than the post-bomb age at 45 cm. Based on a linear interpolation between the post-bomb age, assumed to be 1950 AD, and ca. 1590 AD at the top of unit III, the boundary between units II and I can be crudely estimated as close to ca. 1800 AD. This age is not known as a time of significant climatic change either hemispherically (Jones et al.,

2001) or regionally (Briffa et al., 1995). Therefore, we believe that the distinct, though gradual, change in sedimentary structure (from thinly laminated to bioturbated) at the top of unit II may have a different age. Because a notable warming occurred around the Barents Sea at the beginning of the 20th century (Briffa et al., 1995; Henderson, 2002), we consider this time level, ca. 1900 AD, as a possible age for the transition between units II and I.

Linear sedimentation rate during the 'post-bomb' period (ca. 1950–1997 AD) is at least 0.9 cm/year. Sedimentation rate estimates for the older portion of unit I and unit II depend on an age model for the boundary between them. Based on the two models above, these estimates range from 0.3–0.4 cm/year for unit II and 0.4–1 cm/yr for unit I.

4.2. Grain size

Detailed grain-size distribution was analyzed in 20 samples. The diagram in Fig. 2 shows that sediment is mostly uniform in the contents of fine fractions. The fine clay (<0.001 mm) predominates throughout the core, comprising 41–60% of the total sediment, and the total of the finest fractions (<0.005 mm) makes up 67–84%. We believe that this uniformity in the clay content component indicates that its supply is from a single source, the meltwater discharge of the Shokal'ski Glacier. This conclusion is supported by a similarly uniform composition of clay minerals analyzed in three samples of the <0.001 mm fraction from units I, III and IV. Smectite is almost absent in all samples, whereas, the illite content ranges within 39–42% and that of chlorite+kaolinite is 53–61%. Also abundant are finely dispersed quartz and feldspar grains.

The total of two fractions referred to here as 'silt' (0.05–0.005 mm) varies within the limits 16–33%, with values over 25% common in units II and III, mainly due to a rise in coarse silt fraction (0.05–0.01 mm). Coarse silt prevails over fine silt in this interval causing a slightly bimodal overall grain-size distribution. Along with an elevated content of very fine sand (0.1–0.05 mm), this suggests at least two independent mechanisms contributing to the rapid accumulation of the basal, laminated interval of Unit III.

The coarse fractions (>0.05 mm) make up less than 7% and in most cases less than 2% of the total sediment. Generally, coarse material content of less than 1% characterizes Unit IV. The interval from 5.4 to 5.7 m in the middle of unit IV is somewhat enriched in gravel, which is also reflected in higher rock fragments counts (Fig. 2).

The transition between units IV and III at about 4.45 m (ca. 1400 AD) is marked by an increase in finest sand content (0.1–0.05 mm) culminating in a 4% peak at 3.45 m (about 1470 AD), near the top of a distinctly laminated, rapidly deposited interval. Another characteristic feature of this sediment is the presence of clay pellets, whereas the overall content of coarse sand and gravel is mostly low. Fragments >2 mm occur in low numbers per weight unit (Fig. 2) but form peaks of high accumulation rates that are separated by low-IRD intervals and diminish up-section (Fig. 3).

The upper part of Unit III (2.9–1.75 m, ca. 1500–1600 AD) is characterized by the highest content of coarse material comprised of several spikes with up to 2.5% gravel and 5% sand. Additionally, the interval between 2.0 and 2.4 m (ca. 1540–1580 AD) contains very high numbers of rock clasts >2 mm (Figs. 2 and 3). The non-sorted coarse material dispersed in the silty-clay matrix likely represents ice-rafted debris (IRD). The finest sand may have been deposited by suspension flows, which is consistent with occurrence of a millimeter-scale lamination.

Unit II has a lower content of coarse fractions, mostly below 1% except for two sandy spikes, and low numbers of rock clasts. These patterns indicate a restricted degree of iceberg or sea-ice rafting and low activity of near-bottom suspension flows. A

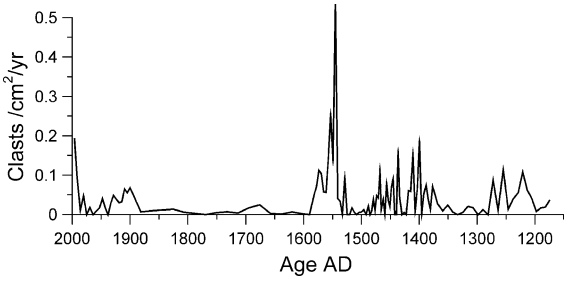

Fig. 3. Accumulation rates of >2 mm rock fragments in ASV-987 versus age. The age of the boundary between units I and II is assumed to be 1900 AD.

low coarse-fraction contents characterizes unit I, whereas accumulation of rock clasts increases at its base (in the 1900 AD age model) and, especially, near the sediment surface (Fig. 3), indicating an intensification of iceberg and/or sea-ice rafting.

4.3. Organic carbon and carbonate contents

Total organic carbon concentration in sediment (TOC, %) and its mass accumulation rates (TOC MAR) are widely considered as important bioproductivity (primary production) proxies. However, on the Arctic continental shelves these proxies may be strongly affected by the contribution of terrestrial organic matter (e.g., Romankevich et al., 2000). The periglacial deserts of northern Novaya Zemlya deliver negligible amounts of soil erosion products, but there is a potential supply of fossil organic matter from black shales drained by the Shokal'ski Glacier. Nevertheless, a comparison of TOC records with other potential proxies of productivity such as foraminifers and macrobenthic remains shows that productivity is probably reflected to some extent in the TOC concentration and accumulation. The TOC distribution in sediment also depends on the preservation of organic matter during sedimentation and early diagenesis. The latter depends on sedimentation rates and redox conditions. Buried organic matter content is higher in reduced sub-bottom environments, which tend to occur when sediment accumulation rates are high.

TOC concentrations in ASV-987 range between 0.26% and 0.68% (Fig. 4a), considerably lower values than in fine-grained Holocene sediments from the open Barents Sea (e.g. Romankevich et al., 2000; Ivanova et al., 2002). TOC MAR values, calculated using the estimated sedimentation rates and TOC percentages, vary within the range of 1–13 mg cm^{-2} $year^{-1}$ (Fig. 4b). These TOC MAR values are at least an order of magnitude higher than those estimated for the open Barents Sea and correspond to the rapid accumulation of fine-grained sediment in the fjord. Therefore, low TOC concentrations mainly reflect a dilution of organic matter by terrigenous material and may not necessarily indicate hindered primary production.

Unit IV is characterized by minor variations in both TOC concentration and TOC MAR (Fig. 4). TOC

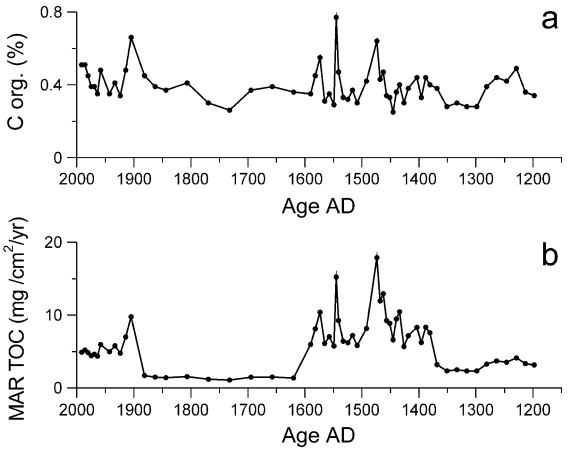

Fig. 4. Total organic carbon content (a) and mass accumulation rates (b) in ASV-987 versus age (age model as in Fig. 3).

MAR rises in the basal laminated sediment of unit III, reaching especially high values of >10 mg/cm^{-2} $year^{-1}$ accompanied by a peak in TOC content at about 1470 AD. After a short decrease in the beginning of the 16th century, both TOC percentages and MAR increased again in the upper part of unit III with two pronounced maxima occurring in black interbeds within a thinly laminated, IRD-enriched interval at ca. 1545 and 1580 AD. The transition to unit II at about 1600 AD is marked by a drop in TOC concentration to <0.4% andin MAR from >10 to 2 mg/cm^{-2} $year^{-1}$.

TOC values are low in unit II, but increase again at the unit II/I transition with a maximum of 0.66% at 0.8 m. Regardless of age model, TOC MAR values are very low in unit II (below 2.5 mg/cm^{-2} $year^{-1}$) and rise in unit I. If we assume the age of the boundary between these units as ca. 1900 AD, the TOC MAR value is almost as high as10 mg/cm^{-2} $year^{-1}$ at the 0.8-m level and diminishes upcore (Fig. 4b).

$CaCO_3$ content in ASV-987 varies in a narrow range between 4.4% and 7.4% without any recognizable pattern other than a slight increase in the upper part of the core. Furthermore, there is no noticeable co-variation of carbonate content with abundances of foraminifers and bivalve shell detritus. This implies additional sources of carbonate such as erosional products from Novaya Zenlya limestones and/or diagenetic carbonate that is commonly formed in reducing environments.

4.4. Macrobenthic remains

Abundances of calcareous bivalve shells (or shell fragments) and remains of chitinous polychaete tubes in the >1-mm fraction have somewhat different distribution patterns, but their major intervals of increased abundances broadly coincide (Fig. 5), presumably reflecting periods of elevated productivity and/or better preservation.

In general, unit IV has the highest frequencies of both macrobenthic components. Their amounts decrease with increasing sedimentation rates at the transition to unit III and reach the lowest levels, with only scarce shell fragments, in the distinctly laminated interval between 3.4 and 4.0 m (ca. 1430–1470 AD). The overlying sediment of unit III contains moderate, varying amounts of macrobenthic remains. Notably, high frequencies of shell fragments occur in intervals between the spikes of coarse rock clasts. In unit II, macrobenthic remains are practically absent, but appear again at the transition to unit I.

4.5. Foraminifera

Planktonic foraminifera are generally rare or absent in ASV-987 except for two samples from unit IV (5.05 and 5.15 m, ca. 1300 AD) and one from the basal part of unit III (4.0 m, ca. 1430 AD). In unit IV

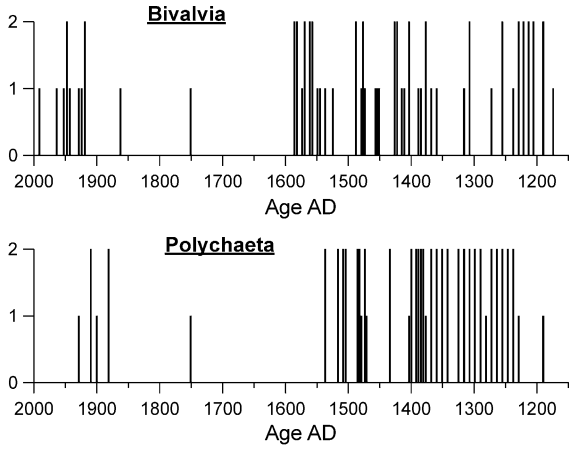

Fig. 5. Relative abundance of bivalve shells and fragments and polychaeta tube fragments in ASV-987 versus age (age model as in Fig. 3). 1—rare, 2—common.

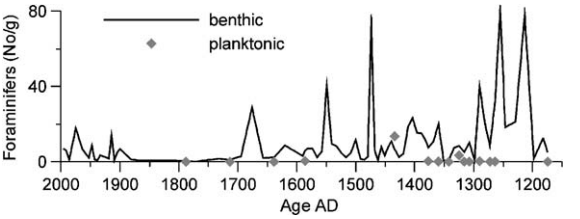

Fig. 6. Benthic foraminiferal numbers in ASV-987 versus age (age model as in Fig. 3).

they are mainly represented by subpolar species *Turborotalita quinqueloba* with minor abundances of *Neogloboquadrina pachyderma* (sinistral and dextral), *Globigerinita glutinata* and *Globigerina bulloides*. In unit III, the polar species *N. pachyderma* (sin.) predominates while *T. quinqueloba*, *N. pachyderma* (dex.) and *G. glutinata* are represented only by a few specimens. We believe that planktonic foraminifera were mostly transported into the fjord from the open Barents Sea by undercurrents (cf. Elverhøi et al., 1980).

The numbers of benthic foraminifera vary between 0 and 80 tests per gram of dry sediment (Fig. 6). The highest values occur in the lower part of unit IV. In other units, benthic foraminiferal numbers rarely rise above 10 tests/g, with several higher spikes in units III and I. The lowest abundances, 0–5 tests/g, characterize unit II, especially its lower part.

Identified benthic foraminifera are represented by 40 calcareous and 4 arenaceous species. Foraminiferal tests exhibit variable preservation conditions. Species numbers vary between 2 and 12 per sample with the highest numbers in units IV and I and lowest in Unit II.

Benthic foraminiferal assemblages throughout the core are strongly dominated by *Elphidium excavatum* forma *clavata* and *Cassidulina reniforme* (Fig. 7). These species are common for Arctic continental shelves including extreme environments such as glaciated fjords (e.g., Hald and Korsun, 1997; Korsun and Hald, 1998). *E. excavatum* f. *clavata* is generally more abundant in units IV through II except for several short intervals, whereas *C. reniforme* mostly predominates in unit I. Several samples, notably in units III and the lower part of unit II contain only these two species.

Among other species, the most interesting patterns have *Nonion labradoricum* and *Cibicides lobatulus*.

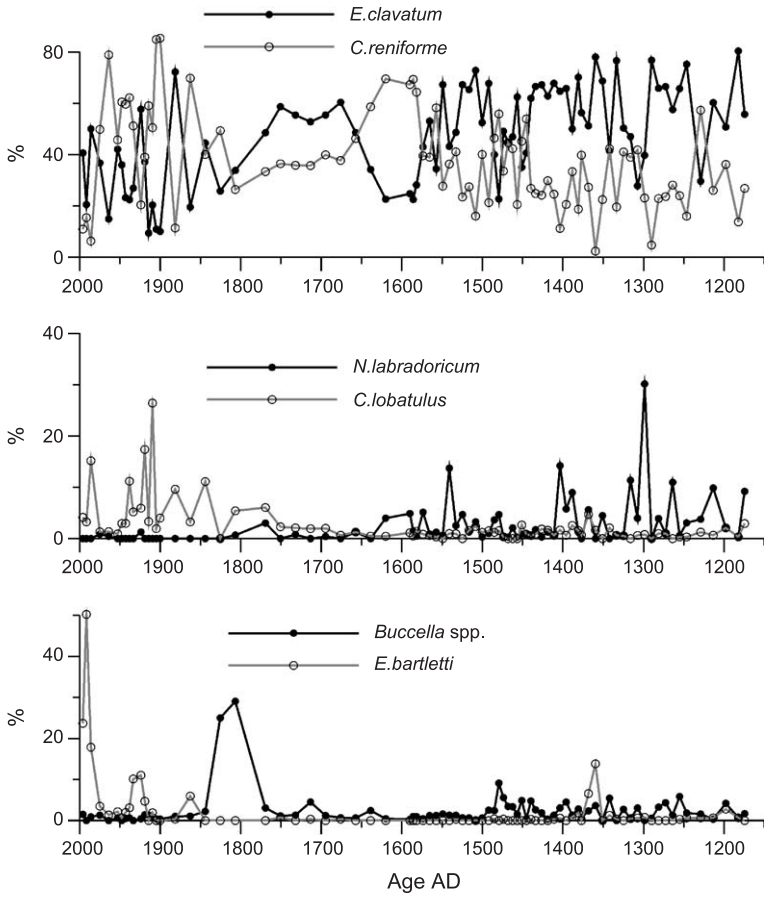

Fig. 7. Percentages of major benthic foraminiferal species in ASV-987 versus age (age model as in Fig. 3).

N. labradoricum, a foraminifer preferring environments with a fresh organic matter input (e.g., Korsun and Hald, 1998; Polyak et al., 2002), reaches high abundances of up to 30% in unit IV and in the upper part of unit III (Fig. 7). The epifaunal species *C. lobatulus*, believed to be related to enhanced bottom hydrodynamic activity (Hald and Korsun, 1997; Polyak et al., 2002), is characteristically present in the upper part of unit II through unit I, where its content reaches >20% (Fig. 7). Additionally, *Elphidium bartletti* is abundant near the core top.

4.6. Stable isotopes

The $\delta^{18}O$ and $\delta^{13}C$ values measured in *Elphidium excavatum* f. *clavata* tests closely co-vary throughout the core (Fig. 7). This indicates that a common control on the composition of both stable isotopes is likely. Equilibrium calcite $\delta^{18}O$ composition calculated from water $\delta^{18}O$ and temperatures measured in September 1998 shows consistent values of 4.3‰ (vs. PDB) for bottom water and as low as near 1‰ at the surface in the fjord interior. This depletion obviously results from high meltwater component. The $\delta^{13}C$ composition of dissolved inorganic carbon in glacial meltwater is also expected to be depleted (Anderson et al., 1983). Therefore, we assume that the concerted depletion in stable-isotopic values in the sedimentary record primarily indicates periods of enhanced glacier inputs to the fjord. Another factor affecting benthic stable-isotopic signature can be the intensity of brines, which help deliver surface water to the fjord bottom. Units III and IV are distinguished by highly variable stable-isotopic values, strongly depleted in both $\delta^{18}O$

and $\delta^{13}C$ at several levels between ca. 1400 and 1500 AD. The upper part of the record shows three distinct depletions including the core top. We note that depleted foraminiferal $\delta^{18}O$ values at the core top appear to be incompatible with normal marine $\delta^{18}O$ composition measured in bottom water in September 1998. A possible explanation of this discrepancy is that the formation of foraminiferal calcite is affected by brines that transport surficial, $\delta^{18}O$-depleted water to the fjord floor later in the fall.

5. Discussion

5.1. Unit IV

Unit IV (ca. 1170–1400 AD) is characterized by a set of sedimentary features that make it distinctly different from the overlying sediments. The lack of distinct lamination, combined with relatively low sedimentation rates (0.6–0.8 cm/year), indicates that the influence of Shokal'ski Glacier on sediment deposition at the core site was subdued. This is consistent with the mostly low content of coarse grains, especially in the upper part of the unit, indicating a limited iceberg discharge, especially given that a portion of the coarse material that is present likely originated from shore-ice rafting. We conclude that the glacier front was only minimally, if at all, extended into the fjord during this time period.

A somewhat different sedimentary environment is evidenced by a distinctly laminated, 40-cm-thick layer deposited in the early 1300s right above an interval with an increased IRD content. These features indicate a possible short-term advance of the glacier front into the fjord, resulting in iceberg rafting and downslope suspension flows (cf. Ó Cofaigh and Dowdeswell, 2001).

Although the content and accumulation rates of organic matter in unit IV are modest, high numbers of macrobenthic remains and foraminifers, combined with an elevated percentage of *Nonion labradoricum* indicate enhanced productivity. Low TOC values possibly result from the intense decay and recycling of organic matter in well-ventilated bottom water that was probably affected by a subsurface inflow from the open Barents Sea. This scenario is also consistent with frequent occurrences of planktonic foraminifers, which are mainly represented by subpolar species.

Overall, the inferred high productivity and retreated position of the Shokal'ski Glacier during the time of unit IV deposition, which corresponds to the late phase of the Medieval Warm Period, suggest relatively warm and/or long summer ice-free seasons. This interpretation is consistent with a generally mild contemporaneous climate in the Northern Hemisphere (e.g., Jones et al., 2001; Bradley et al., 2003) and with elevated summer temperatures in the Nordic seas as reconstructed from proxy data (Andersen et al., 2003).

5.2. Unit III

The transition to Unit III is marked by a dramatic change in sedimentation regime at or slightly before 1400 AD, which generally corresponds to the beginning of the Little Ice Age. The distinctly laminated, 1.15-m-thick basal layer of unit III accumulated very rapidly (at rates between 1.2 to at least 1.8 cm/year) in ca. 70 years. This sediment is characterized by fluctuating, but generally elevated content of very fine sand (0.05–0.1 mm) and the presence of clay pellets combined with low overall contents of coarse fractions and strongly fluctuating accumulation of >2-mm IRD. We suggest that these features indicate prevailing pulsed sediment deposition from suspension flows intertwined with sedimentation events from icebergs, associated with the advance of the glacier front into the fjord. This interpretation is corroborated by the ^{14}C age of ca. 1350 AD obtained from a lateral moraine north of the present margin of Shokal'ski Glacier constraining the maximal age of the last major glacial advance (Fig. 1; Zeeberg, 2001).

Pulses of rapid deposition could be seasonal or multi-annual and were probably controlled by downslope sediment transport at the submarine glacier-front fan and/or by deposition from sediment-laden over- and underflows (e.g., Ó Cofaigh and Dowdeswell, 2001 and references therein). The latter process was possibly enhanced by the cascading of brines associated with sea-ice freezing. This mechanism would also enable the transfer of the depleted stable-isotope signature from the surface to bottom water as reflected in several $\delta^{18}O$ and $\delta^{13}C$ minima in the lower part of unit III (Fig. 8). Normal-marine, heavy stable-isotope values in between these minima indicate efficient

exchange of bottom water with the open sea, probably facilitated by undercurrents (estuarine-type circulation). This is corroborated by the consistent occurrence of planktonic foraminifera, with a spike of planktonics at ca. 1430 AD.

The overall decrease in foraminiferal abundances and, notably, in the frequency of macrobenthic remains in comparison with unit IV suggest a reduction of benthic biota. This is consistent with the composition of benthic foraminiferal assemblages being primarily *Cassidulina reniforme* and *Elphidium excavatum* f. *clavata*, indicating severe environments such as high sediment load and low food fluxes (Hald and Korsun, 1997; Korsun and Hald, 1998, 2000) that were likely related to the proximity of the glacier front. Nevertheless, the TOC mass accumulation rates increase in unit III, which is consistent with the presence of iron-sulfide enriched laminae and relatively high values of enzyme activity measured in this sediment (G. Korneeva, personal communication). These characteristics indicate a relatively high primary production and/or rapid burial of organic-rich laminae by glacigenic sediment (cf. Elverhøi et al., 1980).

Based on the evidence for intense glacial melting and sustained biological productivity, we hypothesize that summer temperatures in Russkaya Gavan' may have still been relatively warm in the early 15th century. This interpretation is consistent with a tree-ring record from Polar Urals, south of the eastern Barents Sea, which shows only a slight temperature decrease at this time followed by a brief warming before a prolonged cooling took place at the end of the century (Briffa et al., 1995). If our interpretation of relatively warm summers is correct, the glacial advance at ca. 1400 AD had to be largely forced by an increase in winter precipitation that is delivered to Novaya Zemlya by the cyclonic circulation originating in the North Atlantic (e.g., Zeeberg and Forman, 2000). A corresponding change in the pattern of the North Atlantic atmospheric circulation at 1400 AD can be inferred from ion contents in the GISP-2 ice-core record (Meeker and Mayewski, 2002). This change was interpreted as a strengthening of winter Icelandic Low that should have intensified cyclonic advection into the Barents Sea and thus triggered a widespread glacier expansion in the region. Indeed, glacier advances/surges occurred at about the same time in Van Mejen fjord on southern Svalbard (estimated between ca. 1300 and 1400 AD: Punning et al., 1976; Hald et al., 2001), Franz Josef Land (ca. 1400 AD: Lubinski et al., 1999), and in Scandinavia (15th century: Matthews, 1991). More studies with detailed age control are needed to define the geography and timing of these events and thus to determine their relationship to changes in North Atlantic atmospheric circulation.

Sediments overlying the basal laminated interval in unit III are characterized by some decrease in sedimentation rates, less distinct lamination, and an increase in TOC content and in numbers of macrobenthic remains. The content of coarse grain-size fractions is variable, with several spikes of sand and gravel. The concentration of >2-mm fragments is very low prior to ca. 1530 AD, but rises dramatically in the upper part of unit III with a pronounced maximum around 1550 AD. The rise in IRD numbers co-occurs with a fine convolute lamination, possibly related to bacterial mats as

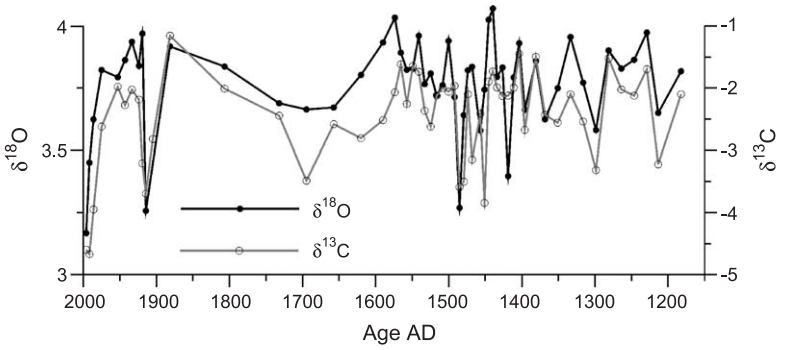

Fig. 8. Stable oxygen and carbon isotope compositions in tests of benthic foraminifer *E. excavatum* forma *clavata* in ASV-987 versus age (age model as in Fig. 3).

well as increases in TOC concentration and the percentage of *Nonion labradoricum* in foraminiferal assemblages. Stable-isotope record shows a distinct depletion in $\delta^{18}O$ and $\delta^{13}C$ prior to 1500 AD succeeded by relatively heavy values. We interpret these features as a stabilization of the glacial front, possibly with an ice shelf extending into the fjord, around 1500 AD and a consequent glacial retreat accompanied by extensive iceberg discharge and enhanced biological productivity. The retreat of Shockal'ski Glacier was probably caused by somewhat warmer summers and/or lower winter precipitation. We note however that the Polar Urals record shows no indication of warming at this time (Briffa et al., 1995).

5.3. Unit II

The transition from unit III to II, at or slightly before 1600 AD, is marked by a three-to five-fold drop in sedimentation rate, depending on the choice of age model for units II and I. Other characteristic features of unit II include overall very low, but slightly increasing up-section, macrofaunal and foraminiferal numbers and organic matter content. Coarse grain concentrations are also generally low, except for two sand spikes in the lower part of the unit. Stable-isotope values are mostly depleted, but become heavier towards the top of the unit. Foraminiferal assemblages are composed of very few species with a predominance of *Elphidium excavatum* f. *clavata* and *Cassidulina reniforme* and rising percentages of *Cibicides lobatulus* near the top.

The combination of these features indicates very low productivity and a limited influence of the glacier on sedimentation in the fjord. This may have been caused by cold and/or short summer seasons and prolonged periods of sea-ice cover. In the context of this interpretation, the depleted stable-isotope signature may be related to persistent formation of brines and/or to an enhanced vertical water exchange due to the weakening of the estuarine-type circulation, which is corroborated by an almost complete absence of planktonic foraminifers. An alternative interpretation of the low numbers of macrobenthic remains and foraminifers, as well as organic matter content, is that they resulted from diagenetic losses because of diminished sedimentation rate. However, low sediment delivery itself likely indicates a reduced influence of glacier melting on sedimentation. In any case, the sedimentary and hydrographic environment was not uniform as indicated by sporadic iron-sulphide enriched interbeds and sandy layers in the lower part of unit II and an overall evidence of improving productivity towards the top of the unit.

The placement of unit II into a wider paleoclimatic context strongly depends on which age model is used for this interval of ASV-987. Generally, the deteriorated environments appear to be in accord with low temperatures observed throughout the Northern Hemisphere during most of the LIA until ca. 1900 AD, with warmer conditions characterizing only the 18th century (Jones et al., 2001). The Polar Urals record (Briffa et al., 1995) also indicates cold summers in the 19th century.

5.4. Unit I

Provided the transition between units II and I occurred near 1900 AD, it was marked by a considerable increase in sedimentation rates. Accompanying changes include generally rising numbers of macrobenthic remains, foraminifers, and organic matter content. The contents of coarse grain fractions remains low throughout the unit, but accumulation of >2-mm fragments increased with increasing sedimentation rate and, notably, at the core top. A noticeable spike in TOC in the basal part of unit I co-occurred with a stable-isotope minimum; another depletion in $\delta^{18}O$ and $\delta^{13}C$ characterizes the core top. Foraminiferal assemblages are more diverse than in unit II and are characterized by a prevalence of *Cassidulina reniforme* over *Elphidium excavatum* f. *clavata* and elevated percentages of *Cibicides lobatulus* and *Elphidium bartletti*, the latter being especially abundant near the core top. We note that high content of *E. bartletti* has been reported in foraminiferal assemblages near the mouths of Siberian rivers, where environments are characterized by a combination of freshwater influence with relatively high productivity (Polyak et al., 2002).

We interpret the changes observed in unit I as an overall increase in biological productivity and an enhancement of glacial melting, both indicating warmer summer temperatures. However, glacier melting did not have such a strong influence on sedimentation in the fjord as during the early LIA (between 1400 and 1600 AD), because of the

retreated position of the glacier front. Our interpretation of warmer conditions in Russkaya Gavan' in the 20th century is consistent with widespread evidence of warming, both globally (Jones et al., 2001) and in the Barents Sea region (Briffa et al., 1995; Henderson, 2002).

6. Conclusions

The high-resolution, multiproxy sedimentary record ASV-987 from Russkaya Gavan', a high-arctic fjord on the northwestern coast of Novaya Zemlya, shows considerable changes in sedimentation rate, degree of lamination and bioturbation, IRD content, numbers and composition of macrofaunal remains and foraminifers, and stable-isotope composition in benthic foraminiferal tests. We interpret these changes in terms of advances and retreats of the glacier front, glacier meltwater discharge and iceberg calving, biological productivity, and sea-ice conditions. The reconstructed paleoenvironments in Russkaya Gavan' based on this record are generally consistent with large-scale paleoclimatic changes from the end of the 12th century to present, encompassing the late Medieval Warm Period, the Little Ice Age, and the 20th century warming.

The late MWP, ca. 1170–1400 AD, was characterized by a limited control of the tidewater Shokal'ski Glacier on sedimentation in the fjord and by relatively high biological productivity indicating warm and/or prolonged summers and a retreated position of the glacier front. Estuarine-type circulation with the penetration of subsurface water from the open Barents Sea episodically developed during this period.

The onset of the LIA at ca. 1400 AD, was marked by a dramatic increase in sedimentation rate combined with a distinct lamination, likely controlled by sediment deposition from glacial meltwater and pro-glacial suspension flows with an advance of the tidewater glacier front into the fjord. We infer that this advance was caused by an increase in winter precipitation rather than cooler summers, which is consistent with a contemporaneous change in the North Atlantic atmospheric patterns reconstructed from the GISP-2 ice-core record. Subsequently (ca. 1470–1600 AD) the glacier-front position stabilized and retreated, accompanied by extensive iceberg discharge and somewhat enhanced biological productivity.

The late LIA period (ca. 1600–1800 or 1900 AD, depending on choice of age model) was presumably characterized by cold summers and extended periods of sea-ice cover, which reduced the influence of glacial melting on hydrographic, biological, and sedimentary environments in the fjord. The latter is especially well expressed in strongly decreased sedimentation rates.

The recent warming in Russkaya Gavan' is assumed to have started at the onset of the 20th century, but this remains to be verified by additional age constraints. Conditions in the fjord during this period featured enhanced productivity and glacial melting, indicating warmer summers.

Acknowledgements

The expedition of r/v *Akademic Sergei Vavilov,* cruise 11, was funded by the P.P. Shirshov Institute of Oceanology, Russian Academy of Sciences. The analytical studies were partially supported by US NSF grant OPP-9725418 to L. Polyak. We are grateful to all people who participated in the collection and processing of core ASV-987. We thank V. Gordeev and A. Vetrov for carbon analyses, V. Serova for clay mineral determinations, V. Kazakova and A. Rudakova for grain-size measurements, D. Ostermann for stable-isotope analyses, and G. Alekhina for help in preparation of figures.

References

Aibulatov, N.M., Matyushenko, V.A., Shevchenko, V.P., Politova, N.V., 1999. New data on structure of lateral suspended matter fluxes in the periphery of the Barents Sea. Geoecology 6, 526–540 (transl. from Russian).

Andersen, C., Risebrobakken, B., Jansen, E., Dahl, S.O., 2003. Late Holocene surface ocean conditions of the Norwegian Sea (Vøring Plateau). Paleoceanogr. 18, 22-1–22-13 Art. No. 1044.

Anderson, T.F., Arthur, M.A., Kaplan, I.R., Land, L.S., Veizer, J., 1983. Stable isotopes of oxygen and carbon and their application to sedimentologic and paleoenvironmental problems. In: Arthur, M.A., et al. (Ed.), Stable isotopes in Sedimentary Geology. SEPM Short Course, vol. 10. Society of Sedimentary Geology, Tulsa, OK, pp. 1.1–1.151.

Bradley, R.S., Jones, P.D., 1993. 'Little Ice Age' summer temperature variations: their nature and relevance to recent global warming trends. Holocene 3, 367–376.

Bradley, R.S., Briffa, K.R., Cole, J., Hughes, M.K., Osborn, T.J., T.J., T.J., 2003. The climate of the last millennium. In: Alverson, R.S., Bradley, R.S., Pedersen, T.F. (Eds.), Paleoclimate, Global Change and the Future. Springer Verlag, Berlin, pp. 105–141.

Briffa, K.R., Jones, P.D., Schweingruber, F.H., Shiyatov, S.G., Cook, E.R., 1995. Unusual twentieth-century summer warmth in a 1000-year temperature record from Siberia. Nature 376, 156–159.

Chizhov, O.P., Koryakin, V.S., Davidovich, N.V., Kanevsky, Z.M., Singer, E.M., Bazheva, V.Ya., Bazhev, A.B., Khmelevskoy, I.F., 1968. Oledeneniie Novoy Zemli (Glaciation of the Novaya Zemlya). Nauka, Moscow. In Russian.

Cronin, T.M., Dwyer, G.S., Kamiya, T., Schvede, S., Willard, A., 2003. Medieval Warm Period, Little Ice Age, and 20th century temperature variability from Chesapeake Bay. Glob. Planet. Change 36, 117–129.

De Menocal, P., Ortiz, J., Guilderson, T., Sarnthein, M., 2000. Coherent high- and low-latitude climate variability during the Holocene warm period. Science 288, 2198–2202.

Elverhøi, A., Liestøl, O., Nagy, J., 1980. Glacial erosion, sedimentation and microfauna in the inner part of Kongsfjorden, Spitsbergen. Nor. Polarinst. Skr. 172, 33–61.

Hald, M., Korsun, S., 1997. Distribution of modern benthic foraminifera from fjords of Svalbard, European Arctic. J. Foraminiferal Res. 27, 101–122.

Hald, M., Dahlgren, T., Olsen, T.-E., Lebesbye, E., 2001. Late Holocene paleoceanography in Van Mijenfjorden, Svalbard. Polar Res. 20, 23–35.

Henderson, K.A., 2002. An ice core paleoclimate study of Windy Dome, Franz Josef Land (Russia): development of a recent climate history for the Barents Sea. PhD thesis, Ohio State University.

Ivanova, E.V., Murdmaa, I.O., Duplessy, J.-C., Paterne, M., 2002. Late Weichselian to Holocene Paleoenvironments of the Barents Sea. Glob. Planet. Change 34, 209–218.

Grove, J.M., 2001. The initiation of the "Little Ice Age" in regions round the North Atlantic. Clim. Change 48, 53–82.

Jennings, A.E., Weiner, N.J., 1996. Environmental change in eastern Greenland during the last 1300 years; evidence from foraminifera and lithofacies in Nansen Fjord, 68°N. Holocene 6, 179–191.

Jones, P.D., Osborn, T.J., Briffa, K.R., 2001. The evolution of climate over the last millenium. Science 292, 662–667.

Keigwin, L.D., 1996. The little ice age and medieval warm period in the Sargasso Sea. Science 274, 1504–1508.

Keigwin, L.D., Pickart, R.S., 1999. Slope water current over the Laurentian Fan on interannual to millennial time scales. Science 286, No. 5439, 520–523.

Korsun, S., Hald, M., 1998. Modern benthic foraminifera off Novaya Zemlya tidewater glaciers, Russian Arctic. Arct. Alp. Res. 30, 61–77.

Korsun, S., Hald, M., 2000. Seasonal dynamics of benthic foraminifera in a glacially fed fjord of Svalbard, European Arctic. J. Foraminiferal Res. 30, 251–271.

Lubinski, D.J., Forman, S.L., Miller, G.H., 1999. Holocene glacier and climate fluctuations on Franz Josef Land, Arctic Russia, 80°N. Quat. Sci. Rev. 18, 87–108.

Matthews, J.A., 1991. The late Neoglacial ('Little Ice Age') glacier maximum in southern Norway: new ^{14}C-dating evidence and climatic implications. Holocene 1, 219–233.

Meeker, L.D., Mayewski, P.A., 2002. A 1400-year high-resolution record of atmospheric circulation over the North Atlantic and Asia. Holocene 12, 257–266.

Mikhaliov, V.I., Chizhov, O.P., 1970. Scientific results of the glaciological investigations on Novaya Zemlya in 1969. Data Glaciol. Studies 17, 186–200 (in Russian).

Ó Cofaigh, C., Dowdeswell, J.A., 2001. Laminated sediments in glacimarine environments: diagnostic criteria for their interpretation. Quat. Sci. Rev. 20, 1411–1436.

Ogilvie, A.E.J., Jónsson, T., 2001. "Little Ice Age" research: a perspective from Iceland. Clim. Change 48, 9–52.

Polyak, L., Korsun, S., Febo, L.A., Stanovoy, V., Khusid, T., Hald, M., Paulsen, B.E., Lubinski, D.A., 2002. Benthic foraminiferal assemblages from the southern Kara Sea, a river-influenced arctic marine environment. J. Foraminiferal Res. 32, 252–273.

Polyak, L., Murdmaa, O., Ivanova, E., 2004. A high-resolution, 800-year glaciomarine record from Russkaya Gavan', a Novaya Zemlya fjord, eastern Barents Sea. Holocene, 14.

Punning, J.-M., Troitsky, L., Rajamae, R., 1976. The genesis and age of the Quaternary deposits in the eastern part of Van Mijenfjorden, West Spitsbergen. Geol. Fören. Förh. 98, 343–347.

Romankevich, E.A., Vetrov, A.A., Vinogradov, M.E., Vedernikov, V.I., 2000. Some elements of the carbon cycle in the Russian arctic seas. Fluxrs of carbon from land, carbon in bottom sediments, elements of the balance. Oceanology 40, 363–372 (transl. from Russian).

Zeeberg, J.J., 2001. Climate and glacial history of the Novaya Zemlya Archipelago, Russian Arctic. PhD thesis, Univ. Illinois in Chicago. Amsterdam: Rozenberg. 174 pp.

Zeeberg, J.J., Forman, S.L., 2000. Changes in glacier extent on north Novaya Zemlya in the twentieth century. Holocene 11, 161–175.